Australian Government
Department of Defence
Defence Science and
Technology Organisation

Bonded Repair of a Gun Carriage Using Electroformed Nickel Reinforcements

Alan Baker, Richard Chester and Richard Solly

Air Vehicles Division
Defence Science and Technology Organisation

DSTO-TR-1930

ABSTRACT

A repair technology based on the use of adhesively bonded electroformed nickel reinforcements was successfully developed to repair the trails of light field guns operated by ADF that had been damaged by fretting or mechanical contact in service. The success was judged by the measured reduction in strain in the reinforced regions (~40%) and the durability of these repairs in service over a period exceeding five years, including three years of active field exercises in a humid tropical environment.

RELEASE LIMITATION

Approved for public release

Published by

Air Vehicles Division
DSTO Defence Science and Technology Organisation
506 Lorimer St
Fishermans Bend, Victoria 3207 Australia

Telephone: (03) 9626 7000

Fax: (03) 9626 7999

AR-013-772
October 2006

APPROVED FOR PUBLIC RELEASE

Bonded Repair of a Gun Carriage Using Electroformed Nickel Reinforcements

Executive Summary

A repair technology based on the use of adhesively bonded electroformed nickel reinforcements was successfully developed to repair the trails of 105 mm light field guns operated by ADF which had been damaged by fretting or mechanical contact in service. The success was judged by the measured reduction in strain in the reinforced regions (~40%) and the durability of these repairs in service for a period exceeding five years, including three years of active field exercises in a humid tropical environment.

The repair approach was based on the composite bonded repair technology previously developed in DSTO to repair ADF aircraft. The nickel reinforcements were shown to be sufficiently durable to withstand the severe mechanical and environmental service conditions experienced by the trails. It is very doubtful, based on the surface damage observed, that composite reinforcements (carbon or boron fibres in an epoxy polymer matrix) would have survived.

Simple methods of analysis were used to estimate the loading experienced by the trails, and later verified by experimental strain analysis. Similarly, simple methods of analysis and experimental testing were used to estimate the effect of the damage and to design the reinforcements.

Electroformed nickel reinforcements with excellent surface matching were successfully manufactured from moulds taken from the damaged surfaces of the trails. Whilst electroforming is a very slow process, it requires relatively low cost equipment and can produce a reinforcement with excellent mechanical properties.

Wedge tests showed that the standard grit–blast silane treatment developed in DSTO for composite bonded repair of aluminium alloy components was a suitable process to provide durable adhesive bonding of the reinforcements with film adhesive FM 73. Finally, methods, based on the use of vacuum bags and electrical-resistance heating were shown to be a suitable procedure for bonding the reinforcements to the trails.

Authors

Dr Alan Baker
Air Vehicles Division

Dr Alan Baker prior to retiring from DSTO was Research Leader Aircraft Materials. On retiring he was given the honorary title of Emeritus Research Leader Aircraft Composite Structures. He continues to particpate in DSTO research in his specialist area through his current position as Program Leader in the CRC for Advanced Composite Structures.

Dr Richard Chester
Air Vehicles Division

Dr Richard Chester is the Research Leader for Aircraft Materials in the Air Vehicles Division with responsibility for both metallic and composite materials research as well as smart materials and forensic engineering. His research interests include durability and damage tolerance of aircraft composite materials and all aspects of composite bonded repair technology including surface preparation methods.

Dr Richard Solly
Air Vehicles Division

In an international career spanning 40 years, Dr Richard Solly has contributed to the science of synthesis of unique molecules, chemical reaction mechanisms, the utilzation of alternative energies, hydrocarbon fuel component reactions and bonding processes for electroformed nickel.

Contents

1. Introduction

This paper describes a study and demonstration program to develop bonded repairs for a Hamel 105 mm light field gun used extensively by the Australian Defence Force (ADF) largely because of its portability. However, the procedures described are of generic relevance to the repair of metallic structures used in severe physical environments.

The weight of the Hamel gun is minimised by the use of high-strength steel hollow tubular and box sections in the carriage assembly (the gun trail), Figure 1. The steel used is a weldable corrosion-resistant precipitation-hardened steel with the specification[1] STA60. Table 1 lists some of the properties specified.

Guidelines provided by the original equipment manufacturer (OEM) state that visible damage to the trail is unacceptable. This is because of the high-impulse loads experienced by the trail when the gun is fired. Thus when visible damage occurs, typically from severe mechanical contact, the trail must be repaired or replaced.

The cost of replacing a damaged trail is significant and this makes repair an attractive option. Repair by welding using a similar alloy as a filler wire is a possibility, but results in a reduced strength caused by over aging of the surrounding region and also to high levels of residual stress caused by thermal contraction on cooling. To restore the original strength the trail would have to be heat treated; however, this process requires a large facility and may lead to unacceptable distortion.

Another alternative is the use of adhesively-bonded reinforcements to recover lost strength and stiffness. Bonded reinforcements (or patches) have been extensively used to repair or extend the life of aluminium alloy aircraft structures[2] as well as much larger steel structures including bridges and ships[3]. In many repair applications, high strength and stiffness fibre composites, generally carbon/epoxy or boron/epoxy (carbon or boron fibres in an epoxy resin matrix), are used. The composites are chosen for the reinforcements as they are highly fatigue resistant and immune to corrosion; importantly, they can readily be formed, at relatively low temperatures and pressures, to the shape of the prospective repair area and then adhesively bonded to form a light-weight structurally efficient reinforcement.

Unfortunately, polymer-matrix composites, although attractive for most repair or reinforcement applications, are prone to damage by mechanical impact or abrasion, so are unsuited to the physically aggressive environment in which the Hamel guns operate.

Structural metals, although lacking many of the attributes of the composites as reinforcements, are a much more rugged option, but generally lack the formability required. There are, however, processes where metals can be formed at ambient temperatures and pressures to provide suitable reinforcements; these include computer numerical control (CNC) machining, rapid prototyping and electroforming.

CNC machining is an excellent option where suitable digitizing and machining facilities are available. But this process is expensive and may not provide sufficient fidelity in some applications. Rapid prototyping, based on sintering metal powders, similarly requires expensive equipment and may not provide the highest level of fidelity; further, the resulting reinforcement will be limited in strength.

In contrast electroforming, the process chosen for this study, produces the highest surface fidelity of almost any metal-forming process and, depending on the process, the resulting material has excellent mechanical properties at modest temperatures.

The electroforming process is similar to electroplating in which ions derived from a metallic anode suspended in electrolytic solution are deposited on a cathode – the work piece. Electroforming differs from conventional electroplating in that the deposit is much thicker and is stripped from the cathode – the mould.

The most usual material electroformed is nickel[4] and the electrolyte used is generally a nickel sulfamate solution; this electrolyte allows rapid deposition of nickel with low internal stress and excellent mechanical properties. The main disadvantage is that electroforming is a very slow process, taking several days to accomplish; the deposition rate is of the order of 0.01mm/ hour. Whilst equipment costs compared with the two previous options are fairly modest, considerable knowledge and skill in the process are required to achieve an acceptable result.

Although considerable emphasis has been placed in this section on the reinforcement, the key issue in bonded repairs is the formation of a strong, environmentally durable adhesive bond. The inability to guarantee the formation of environmentally durable bonds has, far more than any other issue, held back the use of bonded repairs in critical applications[5]. The problem of developing durable bonds lies not with the availability of suitable adhesives, but with the development of effective methods of preparing the surfaces for bonding. Structural metals, as a result of their inherent reactivity with environmental moisture pose a difficult problem – particularly in repair situations.

In a repair situation the surface treatment must be reasonably simple as it often has to be accomplished in relatively primitive conditions, using simple equipment. The treatment itself must not cause corrosion or other problems in surrounding regions or present a health hazard.

This paper describes the type and significance of damage to the gun trails, the design approach for the bonded reinforcements, and then materials engineering aspects, including the manufacture of the reinforcements, development of pre-bonding surface treatments and adhesive bonding of the reinforcements to the gun trails. Experimental strain measurements conducted to measure reinforcement efficiency are then presented. Finally, the current condition of the reinforcement and the status of the trails are described.

2. Damage to the Gun Trails

Gun trails are subject to damage from several sources. An example is fretting or abrasion caused by metal chains used inadvertently to immobilize the trails during transportation. Figure 2 shows a particularly severe example of damage caused in this way to the boss region circled in Figure 1; the damage is somewhat less severe than it appears in the figure as it is highlighted by damage to the paint film. Repair of damage in this trail was not attempted, but a trail with similar but less severe damage, Figure 3, was repaired.

Other examples of damage, shown in Figure 4, likely caused by boulder impact and in Figure 5 caused by abrasion to the trail from metal fittings by contact with metal fittings. Further damage was caused by spikes in the firing platform when the platform was being manipulated for transportation. Whilst, in most cases the damage was quite shallow so did not appear to be a serious threat to the integrity of the trails, on the basis of the advice provided by the OEM, any visible damage is grounds for rejection or repair. However, the sharp grooves caused by the firing platform spikes were smoothed out by sanding to reduce the stress concentration.

Table 2 lists damage to the two trails for which repairs were developed in this program.

3. Estimating Design Stresses

Knowledge of the maximum design stresses is one of the pre-requisites when assessing the significance of damage and designing a repair. In most practical situations this information is unavailable and "reverse engineering" approaches[6] have to be taken to make an estimate.

In the case of the gun trail, the magnitude and distribution of stresses developed are difficult to assess since they depend on several variables, including the size of the charge, the elevation of the gun and the reaction through the trail arms – which will depend on ground resistance.

Estimates of stress in complex components and loading situations are generally made by using finite-element (F-E) modelling, which is a costly procedure and generally requires validation by experimental strain analysis. Unfortunately, effort was not available in this program to conduct an F-E analysis. However, it was particularly fortunate that strain measurements had been made on the boss region during early experimental firings. A more comprehensive experimental strain analysis study was undertaken, this time including the arms, following the application of the reinforcements, mainly to assess reinforcing efficiency.

Thus it was decided to take two independent approaches to estimating design stresses: a) based on materials properties, and b) on the experimental strain analysis, although this was only for the boss region.

3.1 Estimation of Design Stresses Based on Material Properties

A repair should restore the static strength of the component to a minimum level plus a margin of safety. In terms used in the design of aircraft (and the philosophy used here, even through we are dealing with a completely different structure and requirements) the highest load expected to be experienced by the component in its lifetime is called the design limit load (DLL) and the margin of safety is often 1.5 × DLL; sometimes 1.2 × DLL is considered sufficient for a repair. During subsequent service (due to cyclic loading and environmental degradation) it is often mandated that the static strength of the repaired structure must not fall below ~ 1.2 DLL.

DLL, in aircraft terminology, is the load which can be withstood by the structure without significant yielding or permanent deformation and the design ultimate load (DUL) is the load that can be withstood without catastrophic failure. Generally DUL = 1.5 × DLL.

Thus in designing a repair an estimate is required of the DLL in the prospective region of the repair. However, in most practical cases stressing information is very difficult to obtain as OEM design information is generally unavailable and FE modelling and/or experimental strain analysis too costly or difficult to undertake. In critical cases where FE modelling is undertaken its predictions are generally validated by experimental strain analysis[7]; however, this can be more limited in extent than when strain analysis is the only source of design data.

In the absence of OEM or FE/experimental data, a simple reversed engineering approach can be made to estimating DLL based on an estimate of the material yield strength[6].

The least conservative estimate is that the stress at DLL (σ_{DLL}) is the metal yield strength divided by 1.5. The logic in making this estimate is based on the (aerospace) requirement that only local yielding is acceptable at DLL the yield stress could be taken as the stress at DUL. Then yielding would only occur where the stress concentration K_T exceeded the relatively low value of 1.5. For example, K_T is around 3 at the edges of an open hole subjected to direct tension or compression.

An over-conservative assumption is that the stress at DUL (σ_{DUL}) is the material ultimate strength so that σ_{DLL} is the material ultimate strength/1.5 (which is often approximately the yield strength). This assumption implies that at DLL regions with K_T of 1.5 or higher would be stressed to ultimate material strength.

Table 1 lists the assumed properties of the steel used in the gun trail. Taking the yield strength (0.2% proof) to be 800 MPa (the lowest likely value) equivalent to DUL the least conservative estimate of σ_{DLL} is 533 MPa and the most conservative estimate, based on a materials ultimate strength of 990 is that σ_{DLL} is 660MPa.

3.2 Estimation of Design Stresses Based on Strain-Gauge Measurements

Two experimental stress analysis studies were made on the trails by the Army Engineering Agency, Australia, at the Graytown Firing Range in Victoria.

The first study[8] focused only on the boss region using strain-gauge rosettes to estimate the principal stresses. Strain measurements were made at various gun barrel elevations and shot charges. The highest principal tensile stress experienced, based on measured strain, was 324MPa and the highest principal compressive stress was – 258MPa. Thus taking a margin of safety of 20% to allow for the possibility of higher loads not measured in these tests gives 389 MPa as a reasonable estimate for the stress at DLL from these tests.

The second experimental strain analysis <u>made after the application of the reinforcements</u>[9] was more comprehensive since it included the trail arms. Measurements on the arms were mostly made from single gauges, whereas those on the boss region were made from rosettes, as in the first study. The aim of using two guns in the second study was to compare stresses in prospective repair regions with those after implementation of the reinforcements. It will also be shown that excellent agreement was obtained between the two trials in the unreinforced regions.

Figure 6 and Figure 7 present the results for the unreinforced boss and arm regions, respectively, from the second study. Figure 6 shows the principal stresses in the boss region are quite similar to those found in the first study. However, as shown in Figure 7 higher stresses are experienced by the arms; only gauge E1 is a rosette, so the principal stress is recorded. All the other gauges on the arms were single, so the only the stress measured by that gauge is recorded. The highest stress measured was – 439 MPa so on a similar basis (20% margin) the stress at DLL would have been taken as - 527 MPa.

3.3 Assumed Stress Levels

As previously mentioned, only the results of strain measurements on the boss region were available at the time of the design of the reinforcements. Since it was considered intuitively that the stresses in the arms would be significantly greater than those in the boss region the materials-based estimate of 550 MPa was taken as a conservative value for σ_{DLL} for the trail arms and (based on the strain gauge measurements) a stress of 400 MPa was taken as a conservative estimate of the σ_{DLL} for the boss. The second experimental strain analysis provided later justifications for these conclusions.

4. Estimating the Influence of Damage

Complications caused by the highly variable shape of the damage, the structure of the gun trail (in the region of the boss) and the complex loading preclude anything other than a very approximate assessment of the K_T. Unfortunately no readily available solutions could be found for K_T which approximated the geometries of interest in the trail problem. Again

a detailed F-E analysis would have been a much superior approach, but problematic for the reasons previously mentioned.

Taking a very approximate approach, a "ball-park" figure for the stress concentration[10] caused by a shallow elliptical notch or groove in a thin semi-infinite element under direct tension is given by:

$$K_T = 0.855 + 2.21\sqrt{\frac{d}{r}} \qquad (1)$$

where d is the depth of the notch and r the radius of curvature at bottom of the notch.

A further factor F_t is required in estimating the approximate stress in the notch region at DLL, $\sigma_{NotchDLL}$ since the sheet is of finite depth to allow for the reduced section of the skin of thickness t:

$$F_t = t/(t-d) \qquad (2)$$

Thus the approximate maximum stress in the notch is given by:

$$\sigma_{NotchDLL} = K_T F_t \sigma_{DLL} \qquad (3)$$

Based on assumed DLL stresses for the boss and arm region of 400 and 550 MPa respectively, and using the appropriate geometry detailed in equation 3, the peak notch stresses were calculated and are detailed in Table 2.

The values taken for the notch radius r in the Table are estimates based on various assumptions; for example for chain abrasion the diameter of the chain links. As mentioned earlier, sharp grooves made by the firing-platform spikes were smoothed out prior to reinforcement.

This shows that, on the basis of assumptions made in this very simple analysis, stresses exceeding the yield strength of the steel used for manufacturing the trail are possible in rare cases. The stress situation for the unrepaired trails would be of much greater concern if the notch radius r was smaller or the damage of penetration d was deeper.

Fatigue is an important issue that must also be considered when assessing the influence of damage on the structural integrity of the gun trail. The trail is subjected to low-cycle fatigue of several cycles of diminishing load per firing (depending on the degree of damping) which could lead to crack initiation at the base of the notches. Thus it is prudent to ensure that the stresses at stress raisers do not approach the yield stress of 800 MPa.

These estimations are admittedly extremely approximate, but they do seem to bear out the OEMs guidance that visible damage to the gun trail is not acceptable.

5. Reinforcement Design

Since the damage is small compared to the length required to transmit loads from the trail to the reinforcement[11], it is conservatively assumed that the reinforcement has little effect on reducing K_T.

The basic design parameters for the reinforcement are then simply the thickness required to provide the desired strain reduction in the damaged region and the length required to transfer the loads from the trail into the reinforcement.

It is then necessary to check that the adhesive and reinforcement are stressed within their allowable limits, both for static strength and fatigue. To minimise the shear and peel stresses in the adhesive, it is generally necessary to taper the ends of the reinforcement; tapering also reduces the stress concentration in the parent structure at the ends of the reinforcement.

The input parameters are the stresses in the trail and the assumed materials properties for the trail, the reinforcement and the adhesive. A critical assumption in this analysis is that the predominant failure mode in the adhesive is cohesive – failure within the adhesive, not adhesive at the interface of the adhesive and the trail or the reinforcement. For this assumption to be justified, the use of effective bonding processes and procedures are critical.

5.1 Assumed Materials Properties

There are three sets of materials properties to be used in the design process; these are the trail steel, the electroformed nickel and the adhesive. Table 3 and Table 4 respectively provide the assumed design properties for the STA60 steel and electroformed nickel, obtained as described later. Based on our long-term experience with other repairs the epoxy-nitrile film adhesive FM 73 (by Cytec) was chosen for this application; Table 5 provides relevant mechanical properties of this adhesive at ambient temperature. These Tables include the nomenclature used in the analysis.

5.2 Estimation of Reinforcement Thickness

The simplest approach to designing the repair is to make the reinforcement of equal stiffness to the material removed in the damaged region. That is:

$$t_R = \frac{E_T}{E_R} d \qquad (4)$$

where E, t and d refer to Youngs Modulus thickness and nominal notch depth respectively and the subscripts R and T refer to the reinforcement and trail. A more sophisticated approach, not undertaken here, would allow for the load attraction by the stiffer reinforced region.

Based on equation 4 the required thickness of nickel is thus given by 1.23d where the d values are provided in Table 2, which results in a t_R well below one mm in most cases. However, to ensure handleability in the reinforcements and to maintain profile it was decided to choose 2mm as the thickness of the nickel for all reinforcements.

5.3 Static Stress Allowable for the Adhesive Joint

Having chosen the thickness of the reinforcement (t_R) as 2 mm it is important to check that the loads to be transmitted from the parent structure into the reinforcement do not exceed the shear or peel strength of the adhesive. Here (as previously mentioned) the important assumption is made that the lowest stress failure mode in the joint is cohesive failure of the adhesive layer. Adhesive failure caused by environmental degradation at the metal/adhesive interface is potentially a very much weaker mode, which must be guarded against by using effective pre-bond treatments.

The critical region for the joint is generally at the ends of the reinforcement; local strain concentration in the adhesive caused by the notch is ignored as, compared with that experienced at the reinforcement ends, it will be minor. Also the influence of residual stress is not considered as the nickel reinforcement and steel have similar coefficients of thermal expansion. However, there will be a small level of residual stress as the reinforcement can undergo unrestrained expansion during the bonding process, whereas the heated region in the trail will be constrained by the surrounding cool structure[12].

Figure 8 is a sketch of two end configurations for the reinforcement: a) the simplest having no end (90°) taper and b) with suitable end taper. This section considers case a) where simple equations[13] can be used.

The maximum stress σ_{max} that can be carried by the trail without exceeding the allowable capacity of the adhesive in shear for the 90 ° end geometry shown in Figure 8a is given by:

$$\boldsymbol{\sigma}_{\mathbf{max}} = \left\{ \left[2t_A E_T \left(1 + E_T t_T / E_R t_R \right) \right] \left[\tau_p \left(\gamma_e / 2 + \gamma_p \right) \right] \right\}^{\frac{1}{2}} \qquad (5)$$

Where γ_e and γ_p refer respectively to the shear yield strain and strain to failure of the adhesive taken from shear stress/shear strain curves and t_A is the adhesive thickness. Note that the last term in square brackets is the area under the shear stress/ shear strain curve for the adhesive. It is of interest to note that this area stays approximately constant over the working temperature range of the adhesive.

Based on the adhesive properties listed in Table 5 and the values for E_R and E_T listed in Table 3 and Table 4, Equation 5 shows that the allowable stress before adhesive damage exceeds 1000 MPa, thus failure in shear of the adhesive at a static stress σ_{DLL} of 550 or 400 MPa is not anticipated.

However, it is known that the adhesive is more vulnerable to failure under peel stresses which are not well characterised in terms of simple equations. Previous work[14] showed that the magnitude of the peel stress was very similar to the shear stress, and the level of both are greatly reduced by appropriate tapering as illustrated in Figure 8b.

5.4 Experimental Estimation of Fatigue Stress Allowable

It is known that adhesive systems (particularly the bond interfaces) are vulnerable to cracking (disbonding) under cyclic loading – damage seems to result mainly from peel rather than shear stresses. [This fact is illustrated by the much larger fatigue resistance in these joints under compression loading where peel stresses are negative]. Thus it was decided to check the repair durability with some limited tensile dominated fatigue tests, similar to those described in more detail in Reference 14.

Tests were conducted on specimens with configurations similar to those shown in Figure 8. The reinforcement was electroformed nickel but in this case the parent material was 2024 T3 aluminium alloy.

For these tests a flat plate of nickel was electroformed to a thickness of 2 mm. From this plate, twelve specimens were cut each 130 mm long by 20 mm wide. Following the surface preparation outlined later in Section 7, these were bonded with FM-73 adhesive to each face of a central 2024 T3 aluminium adherend 230 mm by 20 mm wide by 6.4 mm thick. Three taper angles at the ends of the reinforcements were investigated, just two specimens at each level: (a) a 90^{o} taper or flat end, (b) a 6^{o} degree (1:10) linear taper, and (c) the FE optimized taper from Reference 15. The optimized taper is non-linear, having a long thin section at the end of the nickel which approximates the end of a linear 3° taper.

Fatigue tests were conducted in a 100 kN Instron test machine under 3Hz tensile cyclic (sinusoidal) loading at a load ratio (minimum/maximum) R of 0.1. The technique used to detect bond failure involves bonding strain gauges to the tip of the reinforcements and monitoring strain response as a function of cycles. Disbond initiation was defined to have occurred when the strain registered by of one of the gauges dropped by 10%.

Commencing at the initial load, 100000 cycles were applied with a strain gauge measurement each 100 cycles. If the output from the strain gauges decreased by less than 10%, the load amplitude was increased by 2 kN and the loading applied for a further 100000 cycles. For a decrease in strain gauge output of more than 5%, digital images of the edges were carefully monitored.

The drop in strain coincided with the formation of a distinct crack of 0.5 mm in length, generally very close to the nickel/adhesive interface.

As expected, it was found that the load in the parent structure for damage formation was increased by tapering, increasing from ~ 18 kN for the 90 ° taper to 27 kN for the optimal taper. The simple linear 6 ° taper performed almost as well (at 25 kN) as the optimum. Using Equation 5 for the 90 ° taper this corresponds to a total fatigue shear strain in the adhesive of 0.27. The 90 °equivalent shear strain for the 6 ° taper and optimium taper 0.67 and 0.77 respectively.
Again using Equation 5, for the 90 ° equivalent strain for t_T = 5.5 mm this gives:

$\sigma_{maxfatigue}$ = 547 MPa for a 90 ° taper

$\sigma_{maxfatigue}$ = 699 MPa for a 6 ° taper

$\sigma_{maxfatigue}$ = 750 MPa for the Optimum taper

Thus, taking into account that σ_{DLL} is nominally the once in a lifetime stress, it can be concluded that fatigue cracking in the bond line should not be a concern; nevertheless, because of the large number of unknowns it was decided the ends of the reinforcements would be tapered to ~ 6 ° to improve the margin on fatigue strength.

6. Electroforming the Nickel Reinforcements

6.1 Preparation of the Moulds of the Damaged Surface

A mould is required to make an electroformed component. The mould, which is made a cathode in the electroplating bath must either be conducting or coated with a conducting layer.

It is important that the electroformed part can be removed from the mould without distortion - this requirement can be a problem with thin electroforms or electroforms of complex shapes. Stainless or chrome-plated steel is a suitable material for making very simple moulds that can be made by machining. For more complex moulds, as required here, formable materials such as plaster or fibreglass may be used; these materials are rendered conducting, generally by depositing a layer of electroless silver.

The first step in making a mould from a pre-existing component is to make a surface cast or 'splash'. In the second step the mould is then made from this splash by making a counter cast in a durable material such as fibreglass (glass-reinforced epoxy or polyester). The splash material itself must be sufficiently durable to allow formation of the mould. Moulding plaster is the most common material used but silicone rubber or casting resins are often more suitable.

An alternative for electroforming reinforcements is to use the part itself as the mould. To take this approach the part must be removable and small enough to fit into the electroforming bath. In a metallic component, areas where the electrodeposited coating is not required are "stopped off" with a suitable paint.

To make the moulds for the two damaged Hamel gun trails all attachments were removed and the coating removed by sand blasting to bare steel. An area equal to the proposed reinforcement size was marked on the trail and two layers of wax sheeting of thickness 0.25 mm to allow for the adhesive thickness were moulded onto the trail. Moulding plaster was then applied over the wax in sufficient thickness to provide structural integrity.

A female fibreglass mould, again of sufficient thickness to provide structural integrity, was reproduced from the plaster mould. The resulting fibreglass mould, Figure 9, was an excellent reproduction of the surface of the trail.

Finally, to make the mould conductive for electroplating an electroless silver conductive film was deposited from an ammoniacal solution onto the fibreglass mould to an area extending approximately two centimetres beyond the size of the required nickel electroform to allow for clean up of the edges.

6.2 Electroforming the Nickel Reinforcements

Electroforming is accomplished in a nickel sulfamate bath heated to 50° C and agitated with air. The mould is the cathode and the deposit (unlike electroplating where the thickness is in the order of microns) is thick in the order of several millimetres. The anode is generally nickel, which is consumed during the process. The nickel sulfamate solution is continuously purified from organic contaminants by circulating over activated charcoal. The ability of an electroplating bath to produce a uniform deposit in a mould with deep recesses is called its throwing power – compared to other nickel plating baths the sulfamate bath is quite good.

Compared with other baths for electroplating nickel, the sulfamate bath produces deposits with relativity low internal stress that are not prone to distortion when released from the mould.

In deep moulds plating uniformity can be improved by several means, including the use of shields and auxiliary anodes and pulsed current. These techniques also minimise the formation of dendrites or nodules at current density hot spots. Software is available to design electroforming systems in complex cases. Since the surface contour of the prospective repair region was relatively shallow no such refinements were attempted for forming the reinforcements.

After a short time (strike) at low current density to build up the conducting coating, nickel was deposited at a current density of one Amp/mm^2 corresponding to a build up rate of 0.01 mm/h. At this rate of deposition electroformed nickel has a fine crystalline structure, resulting in excellent mechanical properties.

During electroforming it was found that several nodules had formed at the edges of the electroform in regions of local high current density – mainly at the outer edges. These were removed by grinding - an extra 20 mm had been included in the length of electroform for this purpose.

Figure 10 shows the resulting reinforcements. Note the high level of fidelity in the larger electroform, including the damage indentation (which ideally should have been filled in prior to making the mould).

Finally, the edges of the electroform were machined to form a linear taper of 6 ° in the long axis and 11 ° in the short axis.

6.3 Mechanical Properties of the Electroformed Nickel

Measurements of stress strain behaviour were made on strips of electroformed nickel using the test procedure set out in ASTM E08. Three of the large reinforcements, Figure 10, were manufactured and two were sectioned in the flat region to provide four specimens which complied with the procedure prescribed in ASTM E08-86a.

These specimens were strain gauged and tested to provide the results listed in Table 6. A fairly wide range of mechanical properties for electroformed nickel are quoted in the literature, probably depending on the deposition variables eg current density, bath composition and operating temperature etc; the properties listed in Table 6 fall well within the quoted range.

7. Surface Treatment Procedures

Previous work on the development of surface-treatment procedures for the repair of aluminium airframe alloys[16] had resulted in a procedure based on the use of grit-blasting followed by use of an epoxy-compatible silane (γGPS) – and, for optimum performance, coating with a suitable corrosion-resistant primer.

Since the grit-blast silane surface-treatment procedure was found to be effective for low-alloy steels (for example the F111 aircraft wing-pivot fitting[17]) as well as other structural alloys it was assumed that it would also be suited for bonding the nickel electroforms to the gun-trail steel.

Grit blasting is an important pre-requisite for the silane-based surface treatment of aluminium alloys. However, as both the nickel and the steel are very much harder than aluminium alloy, alternative methods to grit blasting of activating the metal surface were investigated. The most promising was etching in an aqueous solution of nitric acid. Although, as shown later, nitric-acid etching offered no major advantage over grit-blasting this process would be chosen if grit-blasting facilities were unavailable.

7.1 Measurement of Bond Durability

The environmental durability of the bonds produced by these surface treatments was assessed using the Long-Crack Extension Specimen shown in Figure 11, based on ASTM D3433.

In the test one of the lever arms was made of D6AC steel plated with the nickel from the sulfamate bath, so was a good representation of the nickel electroform. Unfortunately the trail steel was not available for the other lever arm, so D6AC steel was used as a substitute. This is a low alloy steel (composition 0.43 % C, 0.85 % Mn, 0.90 % Cr, 0.75 % Ni and 0.50 % Mo) and is thus not representative of the trail steel. Thus these tests are

representative only of the durability of the bond to nickel. However, other studies showed that the grit-blast silane process was an effective treatment for stainless steel which is more similar in composition to the steel used in the trails.

In the long-crack extension test the specimen is exposed to a 95 % relative humidity at 50° C and, as shown in Figure 11, screws are used to create the fixed displacement of the lever arms to develop the crack driving force $G_{1.}$ From the resulting growth of the crack in the adhesive bond line the Mode 1 fracture energy G_{1c} is estimated as a function of time. Thus the G_{1c} value is a quantitative estimate of fracture energy of the bond line and therefore the instantaneous resistance to bond failure. Figure 12 plots results obtained for the silane process with and without the primer and with prior nitric acid etching or grit blasting.

After some considerable time, growth decreases to a low value then the value of G_{1c} is taken to be an estimate of long-term bond durability. For crack growth which occurs after the initial displacement of the lever arms bond failure is generally mainly interfacial or adhesive, compared with the initial failure which is generally within the adhesive layer or cohesive. However, as adhesive joints are optimally designed to subject the adhesive predominantly to shear loading, $G_{1c,}$ whilst an excellent indicator of bond durability, is of limited value as a design parameter.

The value for G_{1c} obtained for the nickel-coated specimens compares very well with results for aluminium alloys obtained using the grit-blast silane process[18], Figure 13. This is encouraging as the grit-blast silane process has been shown to provide excellent long-term durability with bonded repairs to aluminium alloys[5].

8. Bonding the Reinforcements to the Gun Trails

The reinforcements were bonded to the gun trails using a silicon-rubber heater blanket to heat the structure and a vacuum bag to apply atmospheric pressure. Two layers of FM73 adhesive were cut to the size of the reinforcement and the adhesive was placed over the damaged region of the trail. The heater blanket was placed over the reinforcement with thermocouples to monitor and control temperature and a bleeder cloth was placed over the heater to provide a passage for expulsion of air etc. A nylon vacuum bag was then formed over the assembly and sealed with butyl rubber. The finished vacuum-bag assembly is shown in Figure 14 for the doubler applied to the boss region of the trail. Cure of the adhesive was achieved at a temperature 120° C for four hours under atmospheric pressure.

Prior to actually bonding the reinforcements a test was conducted to evaluate adhesive flow and integrity. This was done by setting up the vacuum bag assembly as just described and placing a layer of release film on either side of the adhesive. Following the cure procedure the adhesive was released and inspected for flow and voids. Figure 15 shows that the adhesive layer exhibited good flow and little voiding

Figure 16 shows the nickel reinforcement bonded to the gun trail in the boss region and Figure 17 shows two reinforcements bonded to the underside of the same region.

Finally, the bead of adhesive at the edge of each reinforcements was sanded to an angle of 30 degrees and to provide environmental protection of the exposed edges a layer of a two-pot epoxy-coating system was brushed over the adhesive bead at the edge of the reinforcement, the reinforcement itself and the trail for a distance of 5 cm around the reinforcement.

9. Reinforcement Efficiency in Repaired Trails

After the reinforcements were applied the two repaired trails were fully reassembled with the guns and, as mentioned in Section 3.2, an experimental strain analysis was conducted by the Army Engineering Agency. Strain measurements were made at seventeen combinations gun barrel elevations and shot charges. Full details of the range of firing conditions are provided in Reference 8 and 9.

Figure 6 and Figure 7 show the positions of the gauges and the maximum (single gauges) or principal (rosettes) stresses in un-reinforced regions, Figure 18 and Figure 19 show the corresponding strains in the repaired regions.

Before analysis of these results it is necessary to consider first the validity of comparing results from the two guns. Table 7 lists ratios for strain readings from similar gauges on the arms of two trails at similar firing conditions. The theoretical value is unity for a perfect comparison; as can be seen from the Table the comparison is remarkably good. Thus the conclusion can be made that comparing reinforced with un-reinforced measurements from the two guns is valid.

The second step is to compare the reinforcement efficiency by taking the ratio of reinforced to un-reinforced. This analysis is provided in Table 8, which shows that the reinforcement produces a strain reduction of at least 40% in each region and that the level of strain reduction in each region is insensitive to firing condition.

10. Current Status of Reinforcements

After a period exceeding five years, including three years of active field exercises in a humid tropical environment and relatively harsh mechanical treatment, the repaired trials are currently in storage in preparation for scheduled refurbishment. The opportunity was thus taken to conduct a simple inspection, which consisted of a detailed visual examination and a tap test.

All the reinforcements appeared to be in excellent condition with no evidence of disbonding – indicating that no fatigue or environmental degradation has occurred.

However, as shown in Figure 20 there is evidence of significant mechanical contact in the form of extensive chips and scratches to the paint scheme. The observation justifies the choice of nickel for the reinforcements; if polymer-matrix composite reinforcements had been used severe damage would almost certainly have occurred. Refurbishment of the trails involves removal of the paint scheme by grit blasting followed by steam cleaning prior to re-coating – this could prove damaging to a polymer composite reinforcement, unless very carefully undertaken. For the electroformed reinforcements, the only caution given is to avoid removal of the epoxy coating at the reinforcement edges – or replacement prior to painting if removal occurs.

11. Conclusions

- A repair technology based on the use of adhesively bonded electroformed nickel reinforcements was successfully developed to repair the trails of light field guns operated by the ADF which had been damaged by fretting or mechanical contact in service.

- The success was judged by the measured reduction in strain in the reinforced regions (~40%) and the durability of these repairs in active use over a period of three years.

- The repair approach was based on the composite bonded repair technology previously developed in DSTO to repair ADF aircraft. The nickel reinforcements were shown to be sufficiently durable to withstand the severe service conditions experienced by the trails. It is very doubtful, based on the surface damage observed, that composite reinforcements would have survived.

- Simple methods of analysis were used to estimate the loading experienced by the trails, and later verified by experimental strain analysis. Similarly, simple methods of analysis and experimental testing were used to estimate the effect of the damage and to design the reinforcements.

- Electroformed nickel reinforcements with excellent surface matching were successfully manufactured from moulds taken from the damaged surfaces of the trails. Whilst electroforming is a very slow process it requires relatively low cost equipment and produces a reinforcement with excellent mechanical properties.

- Wedge tests showed that the standard grit–blast silane treatment was a suitable process to provide durable adhesive bonding of the reinforcements with film adhesive FM 73.

- Finally, methods, based on the use of vacuum bags and electrical- resistance heating were shown to be a suitable procedure for bonding the reinforcements to the trails.

12. References

1. Ministry of Defence, Defence Standard 95-15/Issue 2 30 May 1997
2. Baker A.A., Rose L.R.F, Jones R, Editors, "Advances in the Bonded Composite Repair of Aircraft Structure", Elsevier 2002.
3. IBID Reference 2, Chapter 42 Grabovac I.
4. Watson F and Worn D. K. "Developments in Electroforming Nickel for Engineering Applications", Metals and Materials Technology 1981, **13**, pp 310-314
5. IBID Reference 2, Chapter 22, Baker A.A
6. IBID Reference 2, Chapter 13, Baker A.A
7. IBID Reference 2, Chapter 27, Walker K.F and Rose L.R.F.
8. Army Technology and Engineering Agency Report No LM 3766 1996, Kowalczewski R.G.
9. Army Engineering Agency, Report No LM 4602, 2000, J.
10. "Peterson's Stress Concentration Factors", Pilkey W.D., Wiley and Sons 1997.
11. Rose L.R.F Theoretical Analysis of Crack Patching Chapter 6 in Bonded Repair of Aircraft Structures (Baker A.A and Jones R. eds) Martinus Nijhoff pp 107-173.
12. IBID Reference 2, Chapter 11, Callinan R.J.
13. L.J. Hart-Smith, Analysis and Design of Advanced Composite Bonded Joints, 1974, NASA CR-2218.
14. IBID Reference 2 Chapter 5, P.D. Chalkley, C.H. Wang and A.A. Baker.
15. J. Wang, A.N. Rider, M. Heller and R. Kaye, Theroretical and Experimental Research into Optimal Edge Taper of Bonded Repairs Subject to Fatigue Loadings, International Journal of Adhesion and Adhesives 25, 2005, pp 410-426
16. IBID Reference 2 Chapter 3, D. Arnott, A. Rider and J. Mazza
17. Baker A.A., Chester R.J., Davis M.J., Retchford J.A. and Roberts J.D., "The Development of a Boron/Epoxy Doubler System for the F111 Wing Pivot Fitting - Materials Engineering Aspects" *Composites* **24** (1993), pp. 511 - 521
18. Rider A. and Chalkley P, "Durability of an Off-Optimum Cured Aluminium Joint" International Journal of Adhesion and Adhesives, 24 (2004) pp 95-106

13. Tables

Table 1 Specified mechanical properties for STA 60 Steel

Condition	Softened	Softened	Aged	Over aged
0.2% Proof Stress MPa	430	620	990	800
Tensile min/max	1030	1160	1170 1360	990 1170
Elongation %	20	15	4	8
Hardness	220	240	370 440	300 370

Table 2 Details of damage to the Hamel gun trails and the estimated stress at DLL remote and at the notch

Trail	Gauge Location	Damage Location	Damage Type	Plate Thickness h (mm)	Radius of curvature r (mm)	Damage Depth t (mm)	σ_{DLL} MPa	t/r	K_T	F_T	Notch Stress MPa
1	A4	Upper plate	Chain abrasion	2.6	7.5	0.89	400	0.12	1.6	1.52	983
1	-	Upper plate	Chain abrasion	2.6	7.5	0.22	400	0.03	1.2	1.09	539
1	A5	Boss plate	Chain abrasion	5.2	7.5	0.21	400	0.03	1.2	1.04	511
1	-	Boss plate	Chain abrasion	5.2	7.5	0.43	400	0.06	1.4	1.09	604
2	C1	Radius region	Boulder impact	2.6	10	0.11	400	0.01	1.1	1.04	454
2	B1	Radius region	Boulder impact	2.6	10	0.58	400	0.06	1.4	1.29	714
2	E4	Inner right tube	Spike damage	5.5	4	0.72	500	0.18	1.8	1.15	1031
2	E5	Outer right tube	Strap Abrasion	5.5	40	0.3	500	0.01	1.0	1.06	553
2	D1	Inner left tube	Spike damage	5.5	4	0.37	500	0.09	1.5	1.07	819

Table 3 Design properties assumed for the STA60 Steel

STA 60	Term	Value
Young's Modulus	E_T	200 GPa
Thickness	t_T	2.6 mm plate, 5.5 mm tube
Thermal Expansion Coefficient	α_T	11 x 10^{-6} per °C
Ultimate Strength	σ_{Tu}	990 MPa
Yield Strength	σ_{Ty}	800 MPa
Poisson's Ratio	ν	0.33

Table 4 Design properties assumed for the electroformed nickel

Electroformed-Nickel	Term	Value
Young's Modulus	E_R	163 GPa
Thickness	t_R	2.0 mm (min) plate
Thermal Expansion Coefficient	α_P	14 x 10^{-6} per °C
Ultimate Strength	σ_{Ru}	860 MPa
Yield Strength	σ_{Ry}	605 MPa
Poisson's Ratio	ν	0.33

Table 5 Design properties assumed for adhesive FM 73

Cytec FM73	Term	Value
Shear Modulus	G	530 MPa
Thickness	t_A	0.2 mm
Shear Yield Strength	τ_p	35.5 MPa
Elastic Strain Limit	γ_e	0.062
Failure Strain	γ_f	0.873
Plastic Strain Limit	γ_p	0.811
Poisson's Ratio	ν	0.35

Table 6 Measured mechanical properties for the electroformed nickel

Sample Number	Ultimate Tensile Strength MPa	Elongation	Yield Strength MPa 0.2% offset	Youngs Modulus GPa
1	872	8.40	714	166
2	880	10.03	518	173
3	877	11.69	532	153
4	868		527	156
5	874		572	162
Mean	874	10.04	573	162
STDEV	4.12		73.08	7.13
95% Conf	3.30		58.47	5.70
Allowables	871		514	156

Table 7 Strain ratios for similar gauges on unreinforced regions in the two trails

Firing Ref	A6	D1	D3	E1
1	1.25	0.87	eliminated	0.92
2	0.95	1.01	0.99	1.06
3	1.19	0.94	0.92	0.99
4	1.10	1.07	1.05	1.04
5	0.94	1.01	0.98	0.94
6	1.08	1.02	1.00	1.01
7	1.02	1.05	1.04	1.06
8	1.07	1.03	1.02	1.06
9	1.04	1.02	1.00	1.03
10	0.86	1.03	1.00	0.93
11	1.05	1.08	1.06	1.12
12	0.68	1.03	1.04	1.07
13	1.11	0.99	1.14	1.03
14	0.90	1.03	1.23	1.06
15	0.93	1.08	0.89	1.11
16	1.13	1.04	1.13	1.07
17	0.95	1.04	1.00	1.15
Average	1.02	1.02	1.03	1.04
STDEV	0.14	0.05	0.08	0.06
95% Confidence on average	± 0.07	± 0.025	± 0.042	± 0.032

Table 8 Ratio reinforced/unreinforced for strain gauges in similar regions on the two trails

	Boss					Arm			
Firing Ref	A4	A5	B1	B2	C1	D2	E2	E3	E5
1	0.53	0.33	0.32	0.61	0.59	0.72	0.64	0.80	0.75
2	0.56	0.31	0.33	0.58	0.49	1.07	0.53	0.58	0.63
3	0.64	0.38	0.25	0.56	0.66	0.61	0.59	0.62	0.67
4	0.61	0.40	0.32	0.50	0.48	0.50	0.64	0.56	0.59
5	0.52	0.31	0.28	0.69	0.53	0.74	0.76	0.62	0.66
6	0.59	0.35	0.34	0.57	0.55	0.56	0.56	0.60	0.63
7	0.61	0.41	0.31	0.47	0.43	0.76	0.47	0.57	0.61
8	0.61	0.40	0.29	0.45	0.45	0.39	0.40	0.57	0.61
9	0.58	0.36	0.25	0.54	0.53	0.50	0.51	0.58	0.62
10	0.59	0.39	0.33	0.51	0.45	0.57	0.63	0.63	0.68
11	0.62	0.43	0.33	0.45	0.45	0.57	0.61	0.53	0.58
12	0.53	0.33	0.27	0.50	0.58	0.58	0.77	0.57	0.62
13	0.57	0.41	0.37	0.53	0.48	0.64	0.54	0.58	0.63
14	0.67	0.40	0.26	0.43	0.43	0.44	0.51	0.57	0.62
15	0.65	0.40	0.25	0.45	0.40	0.54	0.57	0.54	0.59
16	0.56	0.36	0.28	0.54	0.55	0.51	0.55	0.56	0.61
17	0.69	0.47	0.27	0.40	0.41	0.32	0.32	0.52	0.57
Average	0.60	0.38	0.30	0.52	0.50	0.59	0.56	0.59	0.63
STDEV	0.05	0.04	0.04	0.07	0.07	0.17	0.11	0.06	0.04
95% CL on average	± 0.024	± 0.021	± 0.018	± 0.036	± 0.035	± 0.027	± 0.055	± 0.030	± 0.021

14. Figures

Figure 1 Hamel 105 mm light field guns in firing position

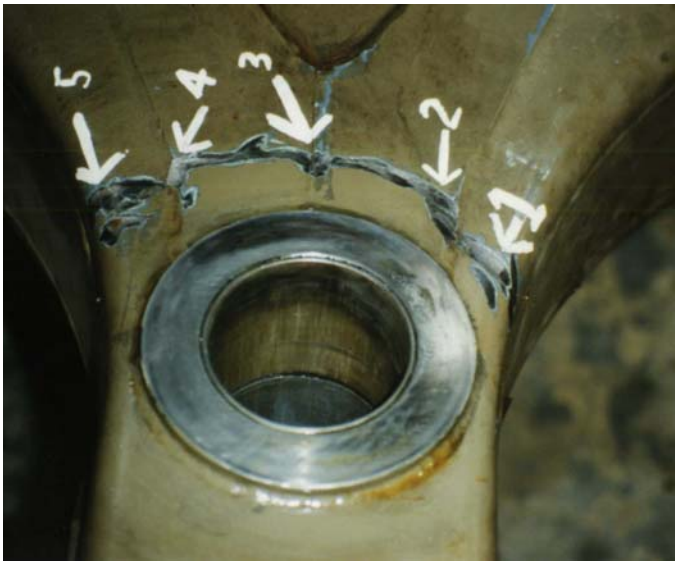

Figure 2 Gun trail showing severe chain scored region ~ 20 mm from boss rim; the region is shown circled in Figure 1- the arms extend from the top of this photograph

Figure 3 Gun trail showing chain scored region, selected for repair study

Figure 4 Gun trail showing damage to the base of the box section selected for repair study

Figure 5 Gun trail showing damage to the arm, selected for repair study

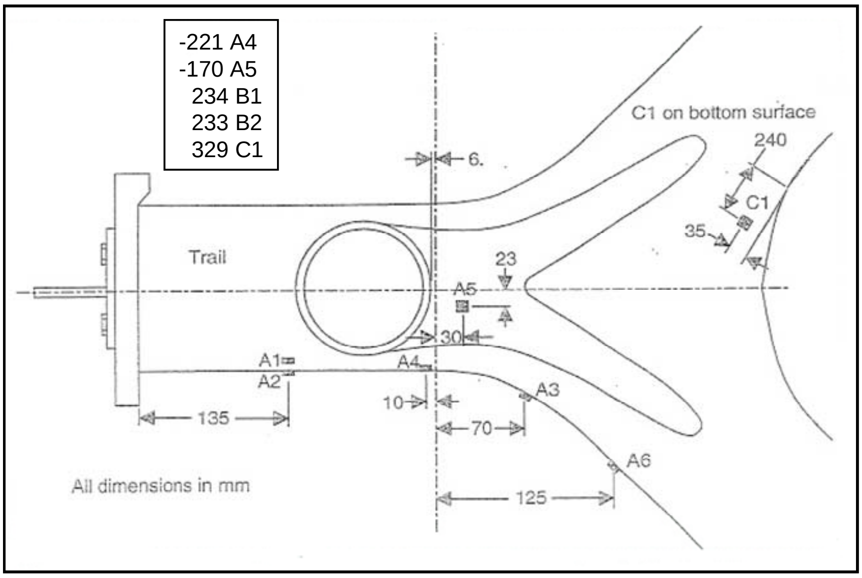

Figure 6 Maximum principal stresses MPa in the boss region of the gun trail, as measured during the firing trials

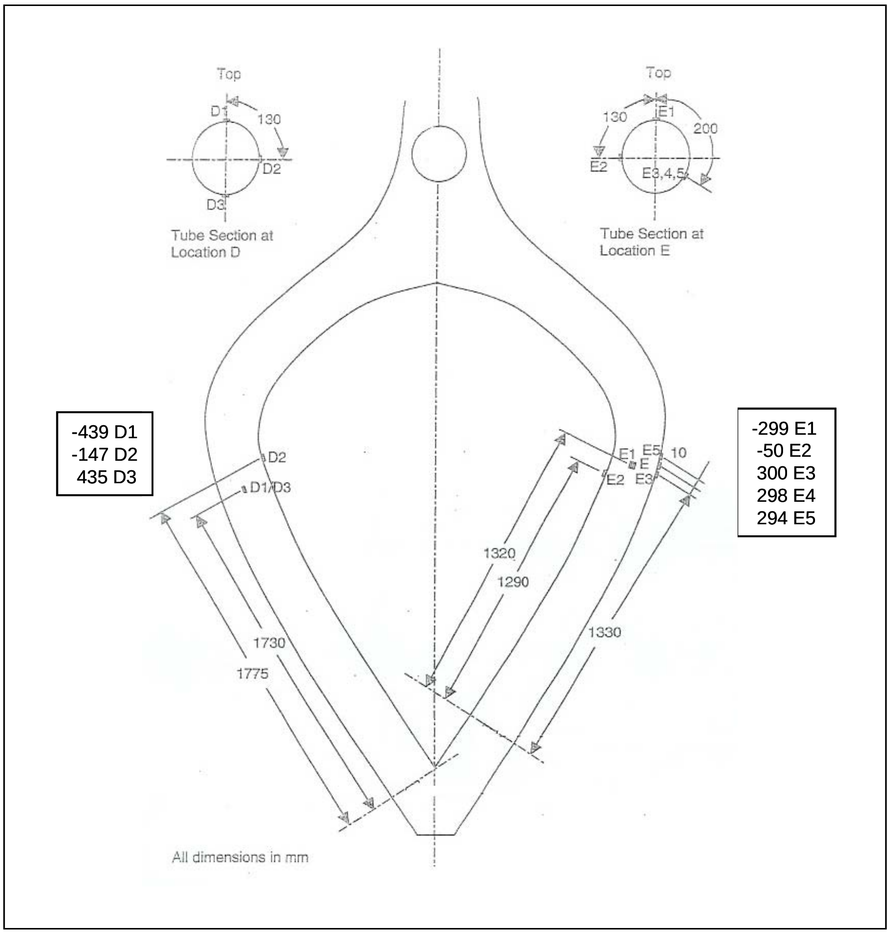

Figure 7   Maximum stresses (gauges D) or principal stresses MPa (gauges E) in the gun trail

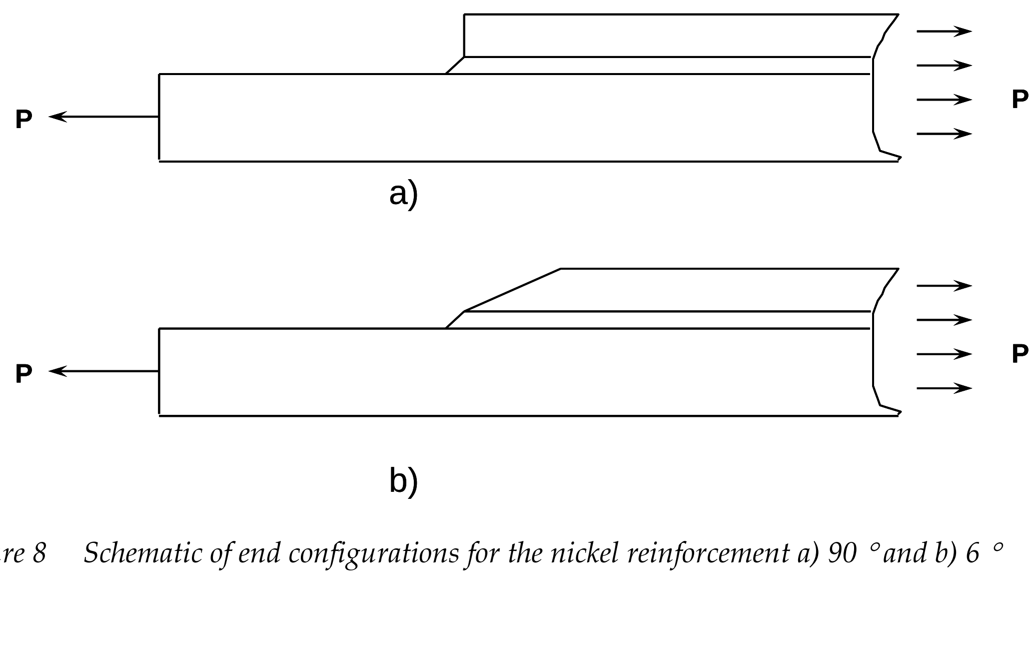

Figure 8   Schematic of end configurations for the nickel reinforcement a) 90 ° and b) 6 °

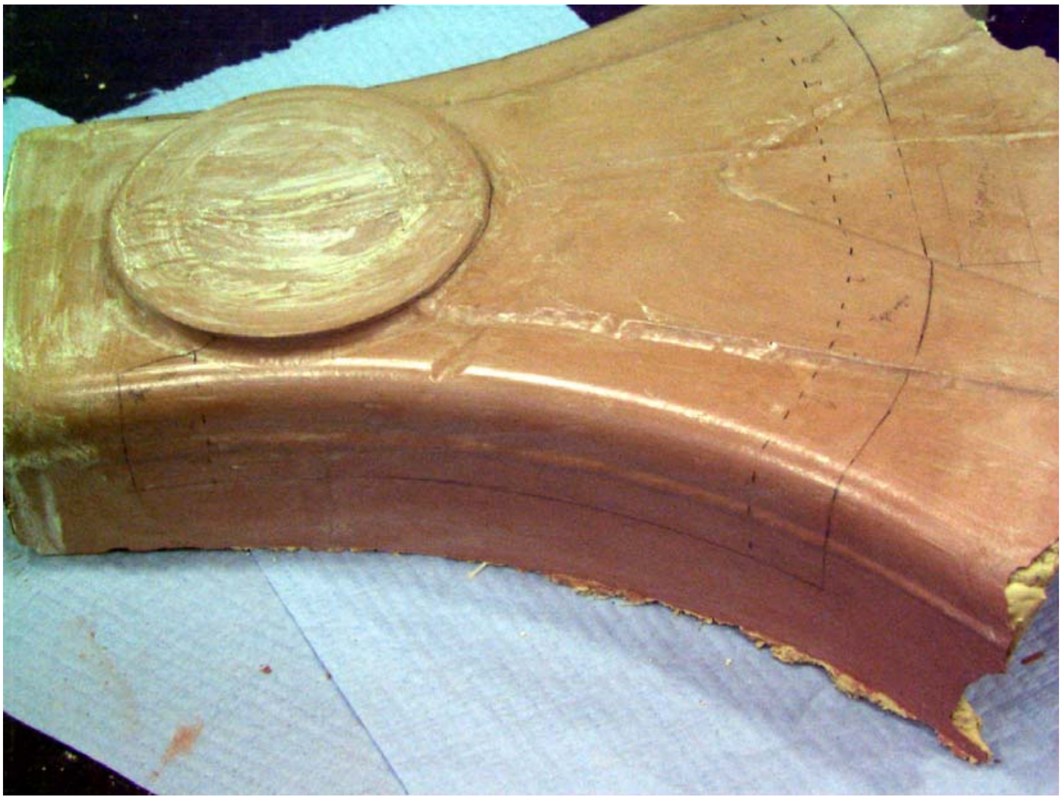

Figure 9 Glass/epoxy mould for electroforming the nickel reinforcement for the boss region of the trail

Figure 10 Electroformed reinforcements, clockwise from the top left regions D, A, E (outer) and B, E (inner) and C

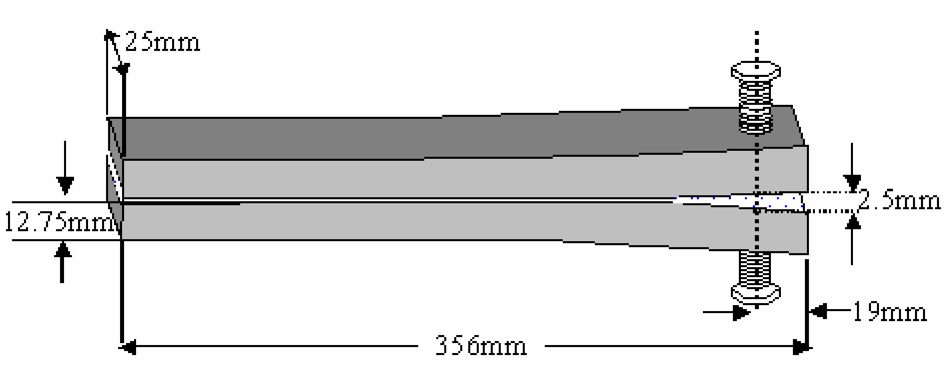

Figure 11   Long crack extension specimen used for measuring bond durability

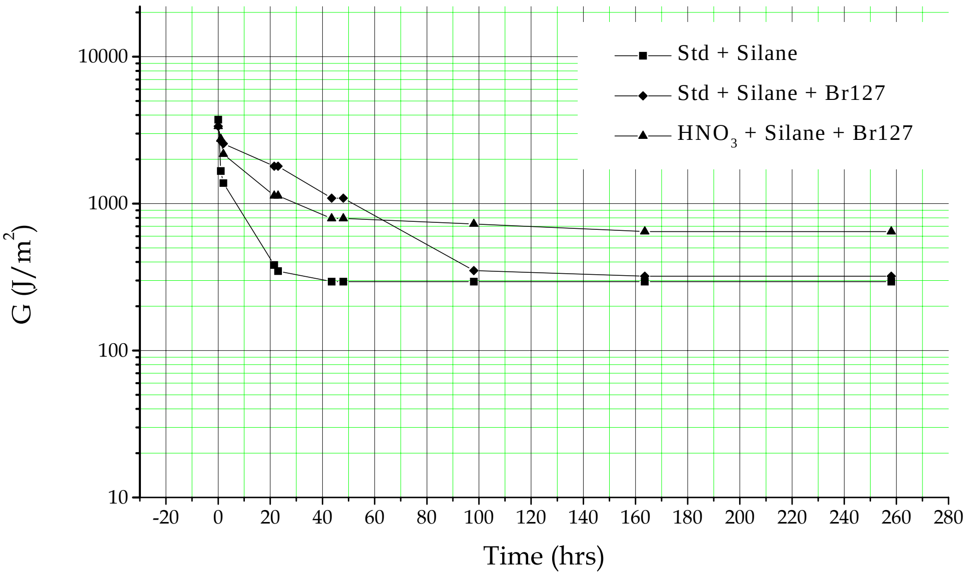

Figure 12   Plot of strain-energy release rate G_{1c} versus time from long crack extension specimens, having one lever arm of D6AC steel plated with nickel and the other bare D6AC

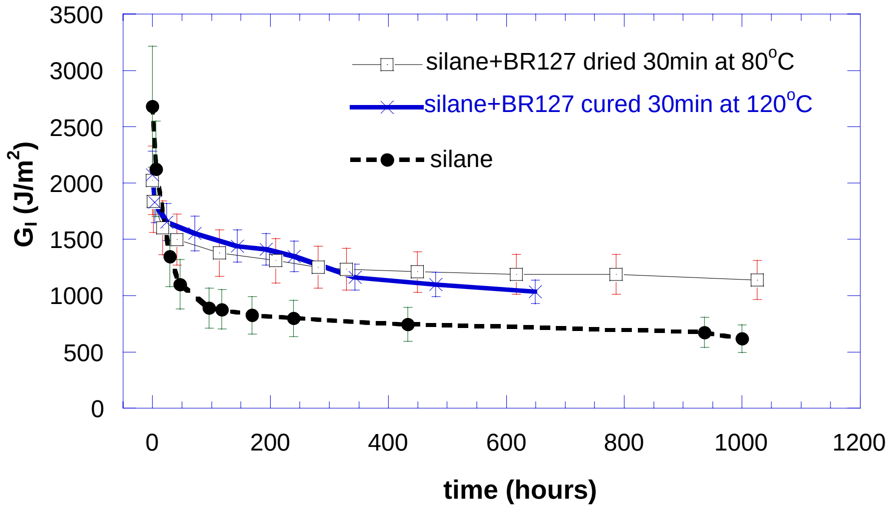

Figure 13 Plot of strain-energy release rate G1c versus time from long crack extension specimens, with 2024 T3 lever arms. Taken from Reference 18

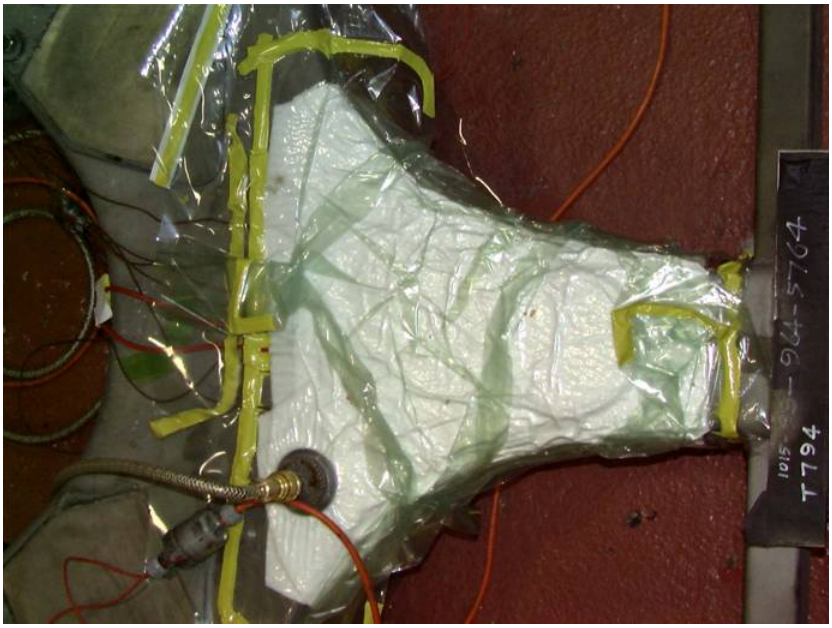

Figure 14 Application of the reinforcement region A in the boss region, showing vacuum bagging assembly

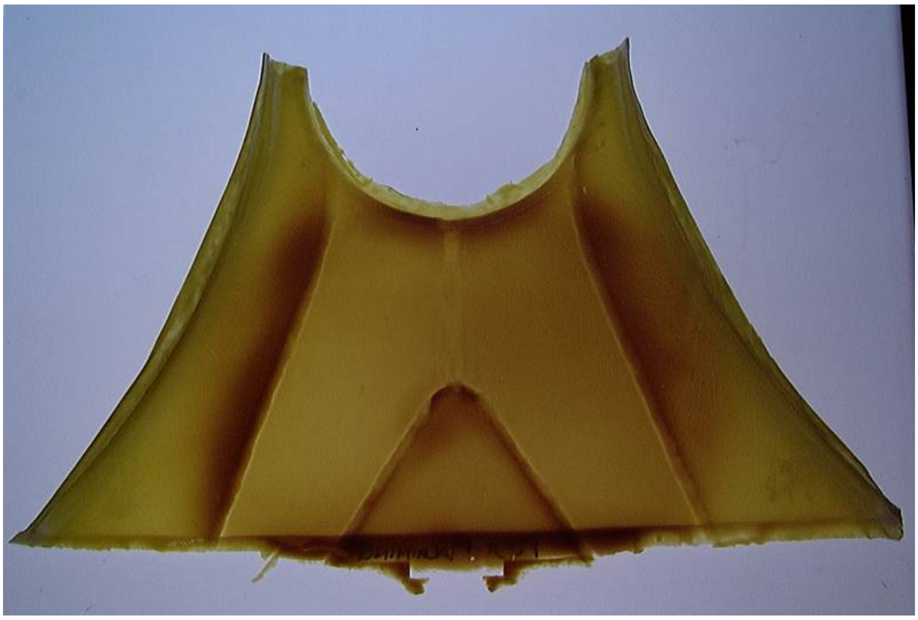

Figure 15   Flow test specimen for adhesive showing excellent flow and low voids

Figure 16   Reinforcement bonded to boss region A

Figure 17   Reinforcements bonded to region C (left and region B right

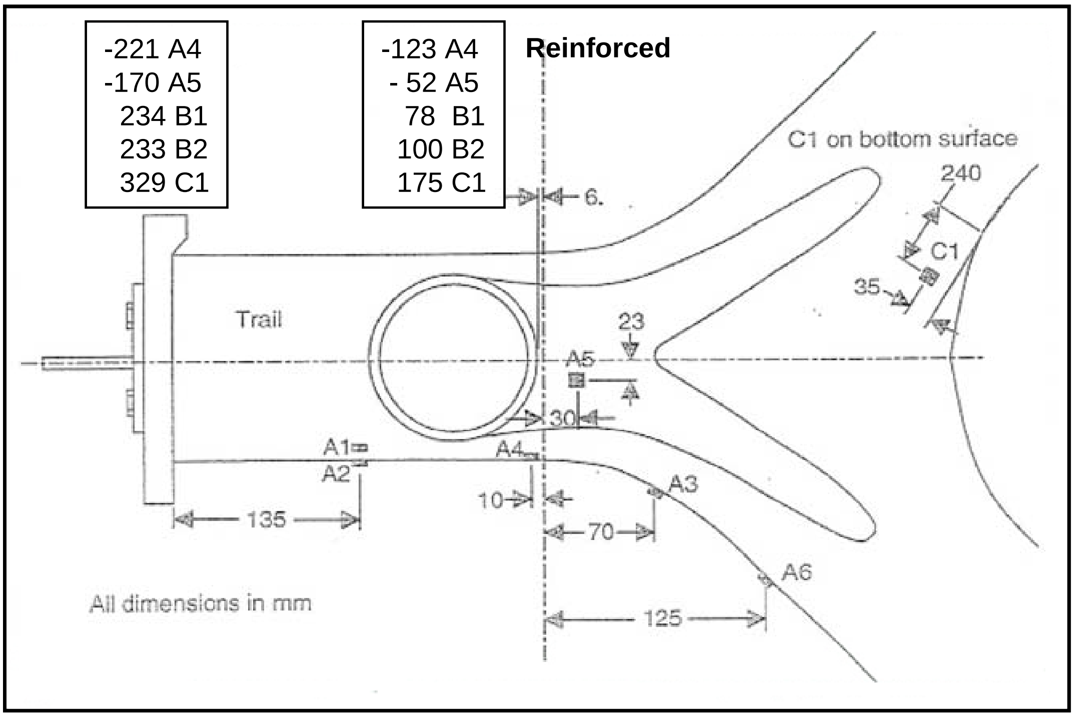

Figure 18   Maximum principal stresses or with and without reinforcements

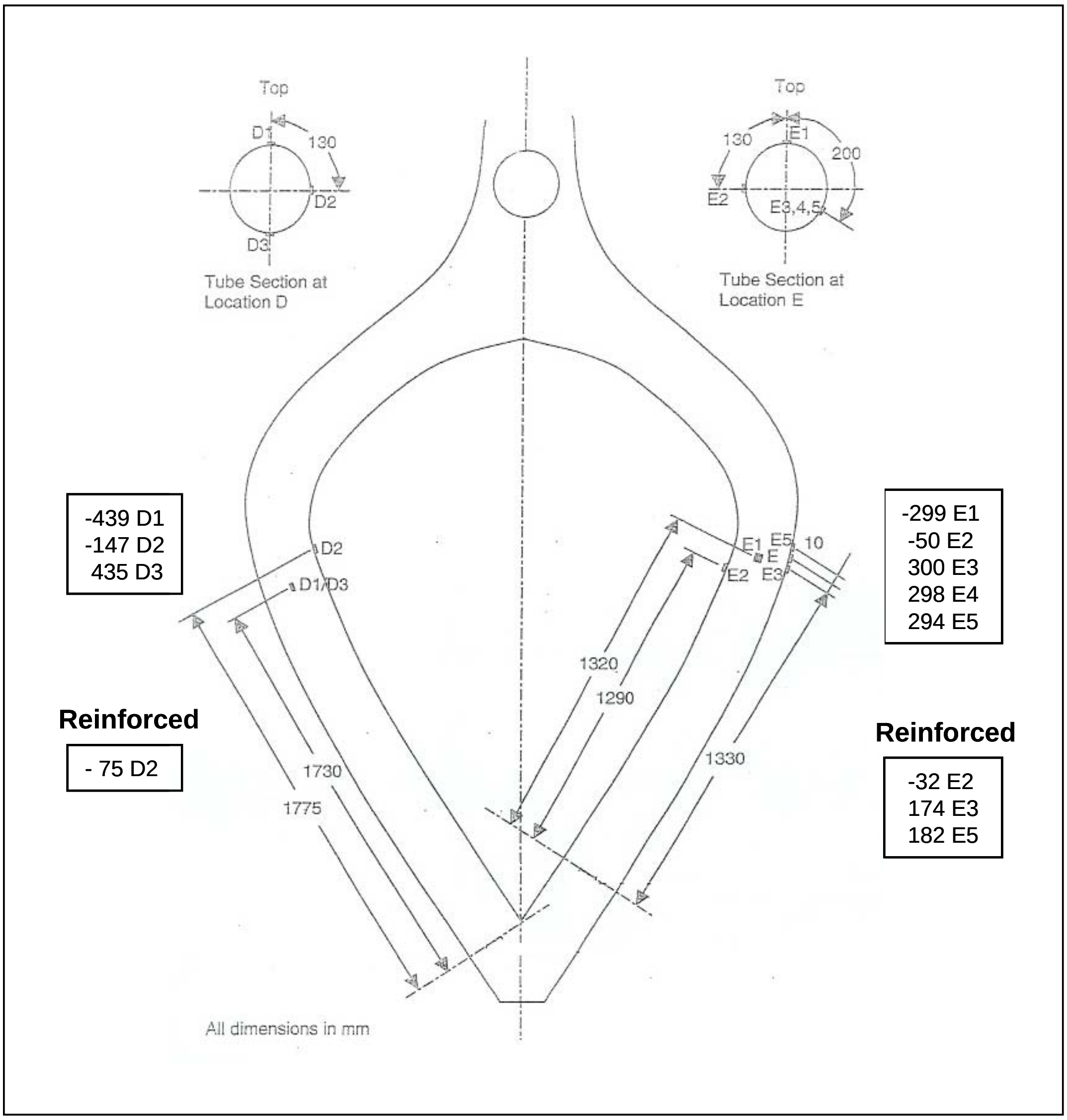

Figure 19   Maximum stresses or principal stresses with or without reinforcements

Figure 20 Reinforcement from region E, showing mechanical damage after three years of active service. No evidence was found of disbonding in this or any of the other reinforcements

DISTRIBUTION LIST

"As per the Research Library's *Policy on electronic distribution of official series reports* (http://web-vic.dsto.defence.gov.au/workareas/library/aboutrl/roles&policies/mission.htm) Unclassified (both Public Release and Limited), xxx-in-confidence and Restricted reports and their document data sheets will be sent by email through DRN to all recipients with Australian defence email accounts who are on the distribution list apart from the author(s) and the task sponsor(s). Other addressees and Libraries and Archives will also receive hardcopies."

Bonding Repair of a Gun Carriage Using Electroformed Nickel Reinforcements

Alan Baker, Richard Chester and Richard Solly

AUSTRALIA

DEFENCE ORGANISATION	**No. of copies**
Task Sponsor	
Mr J. Iannaccio	1 Printed
Mr D. Lang	1 Printed
Mr L. Geraghty	1 Printed
S&T Program	
Chief Defence Scientist	1
Deputy Chief Defence Scientist Policy	1
AS Science Corporate Management	1
Director General Science Policy Development	1
Counsellor Defence Science, London	Doc Data Sheet
Counsellor Defence Science, Washington	Doc Data Sheet
Scientific Adviser to MRDC, Thailand	Doc Data Sheet
Scientific Adviser Joint	1
Navy Scientific Adviser	Doc Data Sheet & Dist List
Scientific Adviser – Army	1
Air Force Scientific Adviser	1
Scientific Adviser to the DMO	Doc Data Sheet & Dist List
Deputy Chief Defence Scientist Platform and Human Systems	Doc Data Sht & Exec Summary
Chief of Air Vehicles Division	Doc Data Sht & Dist List
Research Leader Aircraft Materials – Richard Chester	1 printed
Head Composite and Low Observable Strictures	1
Author: Alan Baker	1 Printed
Author: Richard Solly	1 Printed

DSTO Library and Archives

Library Fishermans Bend	Doc Data Sheet
Library Edinburgh	1 printed
Defence Archives	1 printed

Capability Development Executive

Director General Maritime Development	Doc Data Sheet
Director General Land Development	1
Director General Capability and Plans	Doc Data Sheet
Assistant Secretary Investment Analysis	Doc Data Sheet
Director Capability Plans and Programming	Doc Data Sheet

Chief Information Officer Group

Head Information Capability Management Division	Doc Data Sheet
Director General Australian Defence Simulation Office	Doc Data Sheet
AS Information Strategy and Futures	Doc Data Sheet
Director General Information Services	Doc Data Sheet

Strategy Executive

Assistant Secretary Strategic Planning	Doc Data Sheet
Assistant Secretary International and Domestic Security Policy	Doc Data Sheet

Navy

Maritime Operational Analysis Centre, Building 89/90 Garden Island Sydney NSW Deputy Director (Operations) Deputy Director (Analysis)	Doc Data Sht & Dist List
Director General Navy Capability, Performance and Plans, Navy Headquarters	Doc Data Sheet
Director General Navy Strategic Policy and Futures, Navy Headquarters	Doc Data Sheet

Air Force

SO (Science) - Headquarters Air Combat Group, RAAF Base, Williamtown NSW 2314	Doc Data Sht & Exec Summary
Staff Officer Science Surveillance and Response Group	Doc Data Sht & Exec Summary

Army

Australian National Coordination Officer ABCA (AS NCO ABCA), Land Warfare Development Sector, Puckapunyal	Doc Data Sheet
J86 (TCS GROUP), DJFHQ	Doc Data Sheet
SO (Science) - Land Headquarters (LHQ), Victoria Barracks NSW	Doc Data Sht & Exec Summary
SO (Science) - Special Operations Command (SOCOMD), R5-SB-15, Russell Offices Canberra	Doc Data Sht & Exec Summary & Dist List
SO (Science), Deployable Joint Force Headquarters (DJFHQ) (L), Enoggera QLD	Doc Data Sheet

Joint Operations Command

Director General Joint Operations	Doc Data Sheet
Chief of Staff Headquarters Joint Operations Command	Doc Data Sheet
Commandant ADF Warfare Centre	Doc Data Sheet
Director General Strategic Logistics	Doc Data Sheet

Intelligence and Security Group

AS Concepts, Capability and Resources	1
DGSTA, Defence Intelligence Organisation	1
Manager, Information Centre, Defence Intelligence Organisation	1
Director Advanced Capabilities	Doc Data Sheet

Defence Materiel Organisation

Deputy CEO	Doc Data Sheet
Head Aerospace Systems Division	Doc Data Sheet
Head Maritime Systems Division	Doc Data Sheet
Program Manager Air Warfare Destroyer	Doc Data Sheet
Guided Weapon & Explosive Ordnance Branch (GWEO)	Doc Data Sheet
CDR Joint Logistics Command	Doc Data Sheet

OTHER ORGANISATIONS

National Library of Australia	1
NASA (Canberra)	1

UNIVERSITIES AND COLLEGES

Australian Defence Force Academy

Library	1
Head of Aerospace and Mechanical Engineering	1
Hargrave Library, Monash University	Doc Data Sheet

OUTSIDE AUSTRALIA

INTERNATIONAL DEFENCE INFORMATION CENTRES

US Defense Technical Information Center	1
UK Dstl Knowledge Services	1
Canada Defence Research Directorate R&D Knowledge & Information Management (DRDKIM)	1
NZ Defence Information Centre	1

ABSTRACTING AND INFORMATION ORGANISATIONS

Library, Chemical Abstracts Reference Service	1
Engineering Societies Library, US	1
Materials Information, Cambridge Scientific Abstracts, US	1
Documents Librarian, The Center for Research Libraries, US	1

INFORMATION EXCHANGE AGREEMENT PARTNERS

National Aerospace Laboratory, Japan	1
National Aerospace Laboratory, Netherlands	1

SPARES	5 Printed

Total number of copies: 39 Printed: 13 PDF: 26

DEFENCE SCIENCE AND TECHNOLOGY ORGANISATION
DOCUMENT CONTROL DATA

1. PRIVACY MARKING/CAVEAT (OF DOCUMENT)

2. TITLE Bonded Repair of a Gun Carriage Using Electroformed Nickel Reinforcements	3. SECURITY CLASSIFICATION (FOR UNCLASSIFIED REPORTS THAT ARE LIMITED RELEASE USE (L) NEXT TO DOCUMENT CLASSIFICATION) Document (U) Title (U) Abstract (U)
4. AUTHOR(S) Alan Baker, Richard Chester and Richard Solly	5. CORPORATE AUTHOR DSTO Defence Science and Technology Organisation 506 Lorimer St Fishermans Bend Victoria 3207 Australia

6a. DSTO NUMBER	6b. AR NUMBER	6c. TYPE OF REPORT	7. DOCUMENT DATE
DSTO-TR-1930	AR-013-772	Technical Report	October 2006

8. FILE NUMBER	9. TASK NUMBER	10. TASK SPONSOR	11. NO. OF PAGES	12. NO. OF REFERENCES
2006/1105061/1	ARM 97/094	J. Iannaccio, D. Lang, L. Geraghty	34	18

13. URL on the World Wide Web	14. RELEASE AUTHORITY
http://www.dsto.defence.gov.au/corporate/reports/DSTO-TR-1930.pdf	Chief, Air Vehicles Division

15. SECONDARY RELEASE STATEMENT OF THIS DOCUMENT

Approved for public release

OVERSEAS ENQUIRIES OUTSIDE STATED LIMITATIONS SHOULD BE REFERRED THROUGH DOCUMENT EXCHANGE, PO BOX 1500, EDINBURGH, SA 5111

16. DELIBERATE ANNOUNCEMENT

No Limitations

17. CITATION IN OTHER DOCUMENTS Yes

18. DSTO RESEARCH LIBRARY THESAURUS http://web-vic.dsto.defence.gov.au/workareas/library/resources/dsto_thesaurus.htm

Guns, adhesive bonding, reinforcement and repair

19. ABSTRACT

A repair technology based on the use of adhesively bonded electroformed nickel reinforcements was successfully developed to repair the trails of light field guns operated by ADF that had been damaged by fretting or mechanical contact in service. The success was judged by the measured reduction in strain in the reinforced regions (~40%) and the durability of these repairs in service over a period exceeding five years, including three years of active field exercises in a humid tropical environment.